Future impacts of Urban and Peri-urban agriculture on carbon stock and land surface temperatures in India

U. Srilok Sagar

Department of Civil Engineering, Indian Institute of Technology, Madras, India

Yatharth Singh

Department of Civil Engineering, Indian Institute of Technology, Madras, India

Ashwin Mahalingam[1]

Department of Civil Engineering, Indian Institute of Technology, Madras, India

Teja Malladi
Indian Institute of Human Settlements, Bengaluru, India

[1] **Corresponding Author: Ashwin Mahalingam, Department of Civil Engineering, Indian Institute of Technology, Madras, Chennai 600036, India.**
Email: mash@civil.iitm.ac.in

Future impacts of Urban and Peri-urban agriculture on carbon stock and land surface temperatures in India

U. Srilok Sagar, Yatharth Singh, Ashwin Mahalingam and Teja Malladi

Abstract
Over the last two decades, cities in India have seen significant urban growth accompanied by green cover loss. Recently however, there has been a growing interest in urban and peri-urban agriculture (UPA) in these urban areas. The extent to which UPA mitigates the effects of urbanization is unclear. The present study aims to quantify the impact of UPA in the cities of Chennai and Bengaluru in India. Past trends of urban growth and green cover depletion are used to predict how urbanized Chennai and Bengaluru will be in the future, using CA Markov techniques on GIS data. A survey was then carried out to understand the general perception and growth trends pertaining to UPA. This survey data was then combined with our land use model to predict the growth of UPA in Chennai and Bengaluru in the future. These 'future maps' were then used to quantify the impact of UPA on biomass and land surface temperatures. We find that UPA can play a small, but not insignificant role in augmenting carbon stock and bringing down land surface temperatures and propose that urban development policies consciously include the role of UPA.

Keywords: LULC analysis, CA-Markov models, Urban and Peri-urban agriculture, Land Surface Temperature, Carbon density

1. Introduction

The growth and expansion of urban areas in India has led to an increase in our built environment stock accompanied by several environmental impacts such as the depletion of green spaces, water logging and an increased heat island effect (Nirupama and Simonovic, 2007; McDonald et al 2012; Weng, 2001; Feng et al 2014). This trend is likely to continue and urban India may house nearly 600 million people by 2030 (UN World Urbanization Prospects, 2018). It is therefore important to analyse urban growth trends and their consequences to both predict future environmental impacts, and to decide upon policy interventions that can lead to more liveable futures.

Urban and peri-urban agriculture (UPA) has been touted as a potential solution that counteracts the environmental impacts of urbanization and has been shown to have positive effects on food production, air quality and other aspects of urban life. There is growing evidence that urban and peri-urban agriculture and forestry (UPAF) can play a role in poverty alleviation and potentially reduce vulnerability to climate change (Lwasa et al., 2014; Asomani-Boateng and Haight, 1999; International Development Research Centre (Canada), 2011; Lee-Smith, 2010; Ricci, 2012; Masashua et al., 2009). Urban forestry can improve energy supplies by producing biomass that is an important source of energy as shown in sub-Saharan African cities (Drescher, 2002). Agroforestry also provides shade, which can bring about changes in microclimatic conditions such as air and land temperature (Belsky et al, 1993; VandenKubeldt and Williams, 1992). Agricultural lands and urban gardens increase evapotranspiration, thereby lowering temperatures through evaporative cooling (Corburn, 2009). A study on the impact of urban gardens in Brooklyn, NY in October for instance reported a temperature reduction from -0.2F to -0.9F (ibid). Green spaces have also been negatively correlated with air pollution. Greater spatial aggregation leads to more centralized green spaces, which facilitate the reduction of air pollution and urban temperatures leading to a decrease in the annual averages of PM10 and NO2. (Ku,2020).

Despite these and other related studies as well as the prevalence of urban farming in Indian cities, the impact of UPA in mitigating the environmental impacts of urbanization, and consequently its potential to be used as a policy intervention mechanism for sustainable urbanization is unclear. Quantification of UPA impacts is a necessary first step in overcoming this challenge. This can be done through a variety of measures. This paper focuses on the quantification of 3 major environmental metrics that can be influenced by UPA. These metrics are -

1. Biomass estimation
2. Change in NDVI (Normal Difference Vegetation Index)
3. Change in LST (Land Surface Temperature)

Having extra green cover accounts for an increase in the carbon stock/biomass available in a region (Lwasa et al., 2014). This increased biomass can have an impact on the quantity of fruits and vegetables available in dense urban regions and can also help sequester extra amounts of CO_2 from the atmosphere. The growth of urban areas also affects the NDVI which is a measure of the green cover quality (Parece and Campbell, 2017). While urbanization will reduce NDVI, UPA is likely to increase it. Finally, the impact of land cover change on air quality and LST was reported by Weng and Yang (2006). Local pollution patterns in cities are mainly related to the distribution of different land use and land cover categories, the occurrence of water bodies and parks, building and population densities, the division of functional districts, the layout of transportation networks, and air flushing rates (Weng and Yang, 2006). A higher level of latent heat exchange was found with more vegetated areas, while sensible heat exchange was more favored by sparsely vegetated areas such as urban impervious areas (Oke, 1982). This contributes to the development of the Urban Heat Island (UHI) effect (Kafy, 2019; Di Leo et al. 2016) which has an impact on Land Surface Temperatures.

The objective of this paper is thus to quantify the impact of UPA on Biomass, change in NDVI and change in LST as Indian cities grow, and investigate the extent to which UPA can serve to influence the microclimate of a city. We next present our research design and methodology followed by our results. The paper concludes with a discussion on the quantitative impacts of UPA and its implications to policy.

2. Methodology

Our methodology is divided into 3 steps. Since our objective in this paper is to investigate the impacts of UPA in conjunction with the growth and evolution of cities, we opted for a simulation based approach. Land Use Land Cover (LULC) simulation analysis deals with the change in land use patterns. It tracks the growth or decline of croplands, urban areas, wetlands, forests etc. As a result the first step involved performing a LULC simulation. This involved gathering geo-referenced data from satellite images (LANDSAT) across different time periods as well as regional data such as population density, slope and elevation, commercial areas etc in a given geography. The land cover satellite images were then classified into the following four categories - Built-Up, Green Cover(crops/forest), Water bodies and Other. Trends in land cover change over time were analyzed and used to project land cover patterns in the future, using mathematical techniques that are explained in detail in subsequent sections below.

The second step involved incorporating micro-level data to understand the spatial and temporal growth of urban and peri-urban agriculture since the growth of UPA was not directly apparent from the LULC simulation. This data was captured from a survey and was integrated into the LULC simulation to predict the growth of UPA. The last step consisted of quantifying the impact of UPA through calculating the change in NDVI, LST and Biomass between current and future land cover configurations using established equations.

Each of these steps and their results are now described in detail. Two cities were taken up for this study. The first was Bengaluru, the capital city of Karnataka along with its neighboring districts. A 3600 sq km area was taken for the study. The other city, Chennai, is located on the south-eastern coast of India and is the capital city of the state of Tamil Nadu. The study area taken up was 3834 sq.km which includes the Chennai metropolitan area. Both cities have similar demographics, and serve the IT and other industries.

3. Land Use Land Cover Simulations

Various spatial and temporal techniques such as CA-Markov models and Logistic Regression, have been used in the past by other researchers to predict urban expansion (e.g. Hamad et al, 2018; Rimal et al, 2018; Arsanjani et al, 2013; Liu et al, 2019). We chose to use the CA-Markov model due to its ability to efficiently combine spatial characteristics through Cellular Automata (CA) approaches and temporal predictions using Markov chains. It also can simulate manifold land covers and multifaceted patterns and hence is ideally suited for understanding and predicting future land-use change patterns. To improve the efficiency of our model and the accuracy of our predictions, CA-Markov techniques were combined with Linear regression and Artificial Neural Network/Multilayer Perceptron (ANN/MLP) techniques (Li et al, 2002). Each of these techniques are unpacked below.

Markov model

A first-order Markov model assumes that to predict the state of the system at a future time step t+1, one need only know the state of the system at the current time t. The heart of a

Markov model is the transition matrix P, which summarizes the probability that a cell with land cover type 'i' will change to land cover type 'j' during a single time step.
Consider the present land cover as a matrix $L_{(t)}$ at time 't' and a transition probability matrix P. Then the land cover map at time t+1 as a matrix $L_{(t+1)}$ is given by the relationship

$L_{(t+1)} = P.L_{(t)}$ where P is a probability matrix as shown below

$$P = \begin{bmatrix} P11 & P22 & ... & P1m \\ P21 & P22 & ... & P2m \\ \vdots & \vdots & \vdots & \vdots \\ Pn1 & Pn2 & ... & Pnm \end{bmatrix}$$

Each term Pij in the matrix represents the probability of a transition from state j to state i where i and j both represent different land cover types. The total probability rule can be extended for multiple time periods as well (Plavnick, 2008). The transition probability matrix from state 0 to state 2 is therefore given by the formula,

$$\begin{aligned} P_{20} &= P(L_2|L_0) \\ &= P(L_2|L_1).P(L_1|L_0) \\ &= P_{21} \,.\, P_{10} \end{aligned}$$

Given a transition probability matrix for land cover, an initial land cover matrix and a time period, Markov chains can help predict the land cover composition at the end of this time period. (Hua, 2017; Huang et al, 2015)

Cellular Automata (CA) model

The spatial influence of various land use types in predicting the land use cover is modelled by a Cellular Automata model. While Markov models give us a global distribution of land cover types, CA models allow us to localize and determine which cells in a space correspond to a particular land cover type (Mitsova et al, 2011; Guan et al, 2011) This model treats land cover as a lattice with individual pixels / cells being called an automaton. The cellular state represents the land use type. A cell together with its surrounding cells is a neighborhood. The state of each cell is influenced by the surrounding cells. The state of each cell at a point in time is given by the following equation.

$$\{S_{t+1}\} = f(\{S_t\} * \{I_{th}\} * \{V\})$$

$\{S_{t+1}\}$ and $\{S_t\}$ are the states of the cell in the CA at time t + 1 and t, $\{I_{th}\}$ refers to the neighborhood where h is the neighborhood size, $\{V\}$is the suitability of a cell and f is a function that denotes the transition rules. Beyond the influence of neighboring cells, the CA model determines land use type as a function of several input variables. For example, the population density, slope, road network, distance to the business districts, location of water bodies etc. play a role in determining the land use cover. For instance, the greater the population density, the more the urban growth will be while a more uniform slope of population growth may promote agricultural land. Based on these factors and rules, change in land cover is modeled over time.

Artificial Neural Network, Multilayer Perceptron (ANN/MLP) model

The ANN/MLP model augments the CA model and allocates pixels to each land cover category based on a probability map. The probability map is derived from the input variables mentioned above (land characteristic maps such as slope, elevation, population density). This model performs various land use transitions simultaneously and works on the principle of training and testing data. We first categorize the 4 land-use classes – green, built-up, water and other uses into 8 parts - 4 transition classes and 4 persistent classes. The ANN/MLP constructs a network of neurons between the input values from the explanatory variables and the eight output classes (the transition and persistence classes) and a web of connections between the neurons that are applied as a set of (initially random) weights.

The ANN/MLP sub-model we used consists of 1 input layer, and several hidden layers that lead to an output layer. The training process involves training 50% of pixels taken from both transitioned and persisted pixels to understand which combination of explanatory variables leads to a change in land cover. This understanding is then tested on the remaining 50% for validation and assessment. Once validated, the ANN/MLP uses these rules to affect land cover change.

Taken together, the Markov model allows us to understand how the various land cover categories change over time through the use of transition matrices. The CA model then uses cell transition rules to allow us to accurately distribute these land cover types spatially across our map, taking into account explanatory variables such as population density, elevation etc as well as neighborhood effects of cells. The ANN/MLP algorithms optimize this process by ensuring that the model learns through iterations and then applies these learnings to simultaneously change land use over time, consistent with the constraints given by the Markov and CA approaches. These approaches were therefore combined to develop our LULC simulation.

Data for the Simulation

The data required for the LULC portion of this study were obtained from raster maps of Chennai and Bengaluru. For the city of Chennai, land cover maps for the years 1997, 2009, 2017 and for Bengaluru land cover maps of 2011, 2016 and 2020 were obtained. These maps were extracted from LANDSAT-4 images. A maximum likelihood function was used to convert the map data into four different land categories – Urban Built-up, Green, Water and Other (barren). Each of these land categories was given a unique value – Urban Built-up (1), Green (2), Water (3) and Other (4). Figure 1 shows the maps that we obtained for Chennai and Bengaluru.

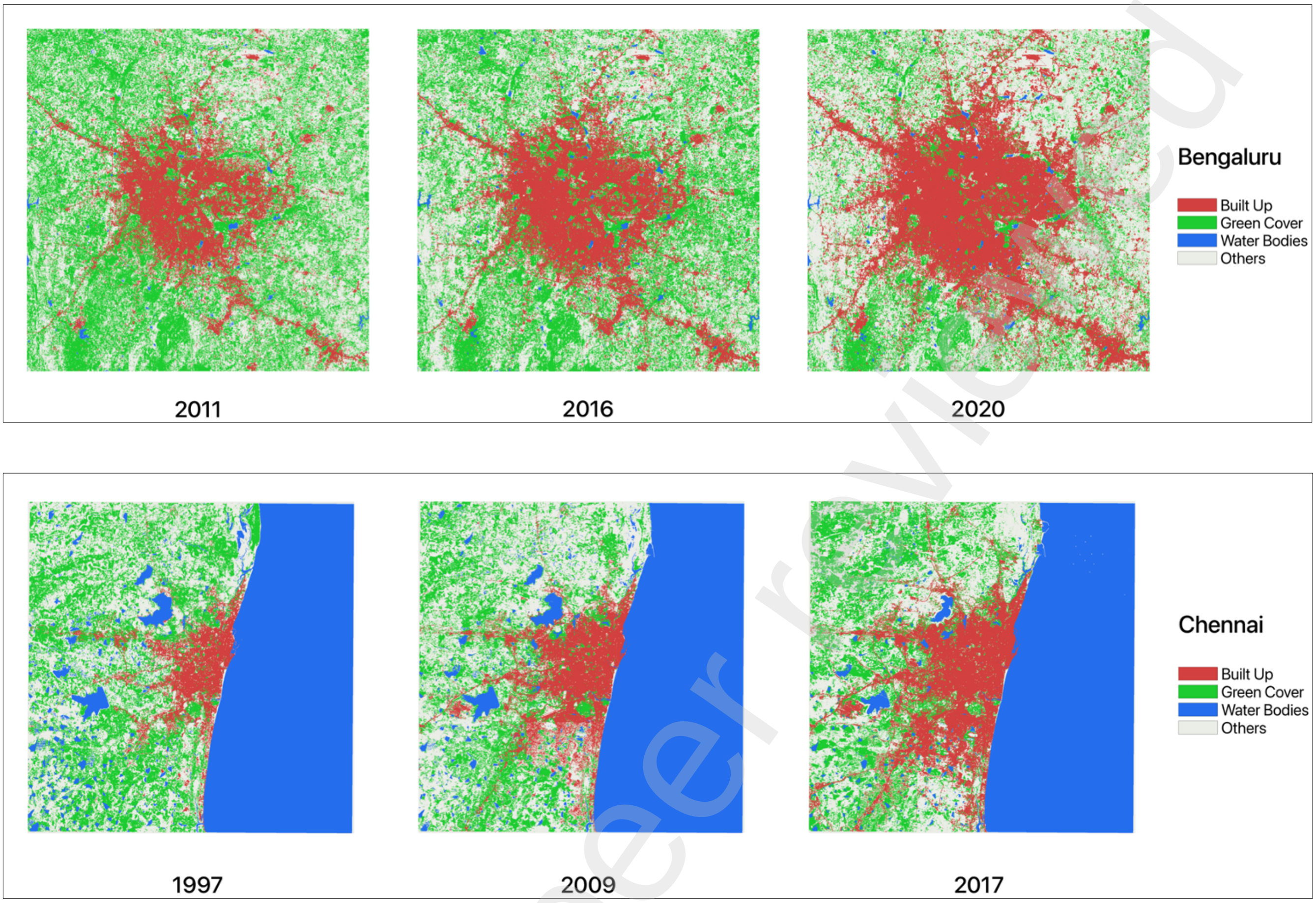

Figure 1. Base maps for Bengaluru and Chennai

Data for a set of variables, namely Slope, Elevation and Population Density, and Restricted areas were downloaded from various sources such as the Global Human Settlement Layer (GHSL) and Open Street Maps (OSM). The values for other variables such as the distance to the nearest road (Euclidean distance from each pixel to the major roads) and the distance to the urban area (Euclidean distance from each pixel to the urban area – central part of the map) were calculated based on data downloaded from these sources using Euclidean distance formulae. Some of these maps are shown in Figure 2 below.

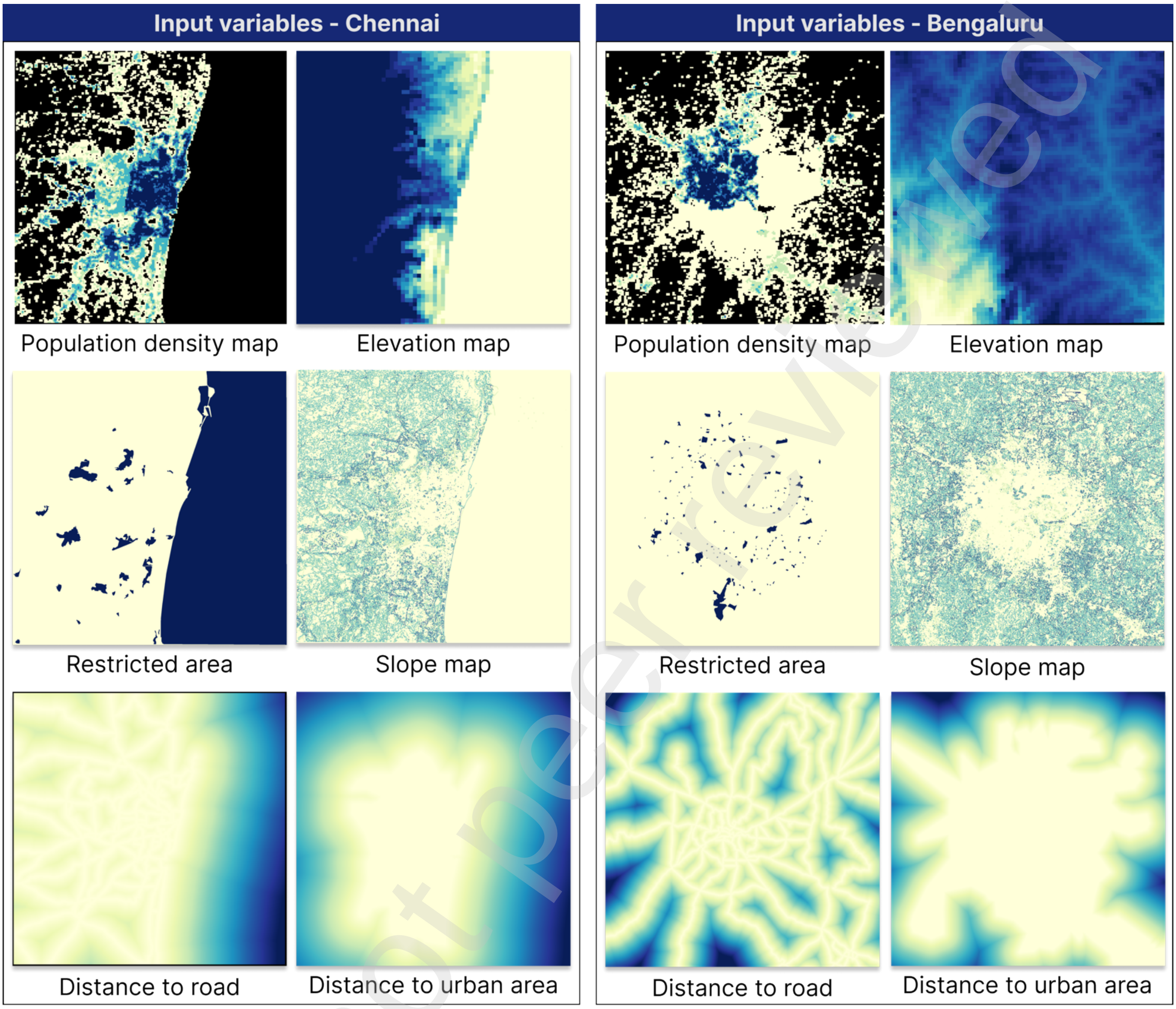

Figure 2. Input variables for Chennai and Bengaluru

Model Development

The initial LULC analysis was performed by grouping pixels with identical values and finding out the number of pixels for each integer value. Each pixel/cell represents an area of 30x30 m in real life. Using this the total area of each land cover category can also be calculated. The 2011 and 2016 maps for Bengaluru were then compared as were the 1997 and 2009 maps for Chennai to determine the number of pixels that were converted from one land use category to another. The results were expressed in matrix form. By dividing each of these values by the total pixels, we obtained a Transition Probabilities matrix for each city.

The transition probability matrix for Chennai is shown in Table 1 below. This matrix represents the probability with which each land use category is likely to be converted into another category. As an example a land cell in Chennai of category 2 (green space) in 1997 is likely to change into category 3 (water) in 2009 with a probability of 0.00953.

Table 1. Transition probability matrix for Chennai from 1997 to 2009

	1	2	3	4
1	1.0000000	0.0000000	0.0000000	0.0000000
2	0.0746224	0.5191057	0.0095304	0.3967415
3	0.0014982	0.0143374	0.9619718	0.0221927
4	0.0882943	0.2466762	0.0187241	0.6463054

Once a base year and a transition probability matrix has been established, the total number of cells of a particular land cover type at a future point in time can be estimated. However it is vital that these cells be distributed across the landscape in a realistic fashion. This special distribution is accomplished through the Cellular Automata model. Here raster maps are developed for each of six different land features - population density, slope, elevation, distance to the nearest road, distance to central business district, and restricted areas. These are treated as the input variables that influence land use change. An actual land use map in the future is fixed as a target, and the CA model in combination with the ANN/MLP module iterates between coefficients for these variables that lead to a land use distribution that best matches the distribution in the future land use map. Finding these coefficients can be done via a number of methods, the most prominent being the MCE (Multi Criteria Evaluation) approach where each land feature map is given a certain weight while predicting the future pixels of a land use category. For example, for predicting the urban growth, the population density map may be given a higher weight at the outset than other maps in predicting the outcome. Similarly for predicting the change in croplands the slope map may be given a higher weightage. These weights are then multiplied up to each land feature map and a transition potential/suitability map is generated. These are the final processed maps that are used to simulate land use changes in future periods.

The CA Markov analysis was done using PLUS - a raster-based Cellular Automata (CA) model for land use/land cover (LULC) change simulation. The PLUS model integrates Land Expansion Analysis Strategy (LEAS) and Cellular Automata Random Seeds (CARS). The LEAS module investigates the underlying transition rules for future land cover simulations. The CARS module uses cellular automata to perform the simulation (Liang et al, 2021).

Random Forest Regression techniques were used in the LEAS module to iterate between input variables and a land expansion map to create development potential maps for each land cover type (Urban Built-up, Green, Water, Other). These maps represent the likelihood of each pixel developing into the corresponding land cover type. In the CARS section, the land use map of the initial period, the development potential maps from the LEAS model, constraint maps, Land demands, Transition Matrix and Neighborhood weights are used to develop a predicted Land use map.

Modeling and Validation

The following constraint matrices represented in Tables 2 and 3 were also used to prevent unviable transitions (e.g. urban built-up areas transitioning into water bodies) where 1 indicates transitions that are allowed and 0 indicates transitions that are not allowed. These matrices lead to two scenarios, one in which green spaces can transition into unused spaces and another in which this transition is not allowed.

Table 2. Transition rule matrix 1

Past to Future	Urban	Green	Water	Other
Urban	1	0	0	0
Green	1	1	0	1
Water	0	0	1	1
Other	1	0	0	1

Table 3. Transition rule matrix 2

Past to Future	Urban	Green	Water	Other
Urban	1	0	0	0
Green	1	1	0	1
Water	0	0	1	1
Other	1	1	0	1

The values of the weights shown in Table 4 correspond to the hierarchy in which the neighbourhood effects take place. For example, in a 3x3 neighborhood, out of the 8 pixels that surround a pixel if there are 3 urban pixels (weight = 1) and 3 green pixels (weight = 0.25), then the pixel will be allotted the urban land cover value as the weight is higher. The scenarios were developed through an iterative process. In total, there will be 4 different scenarios for each city based on 2 different transition rule matrices and 2 different sets of weights.

Table 4. Weights/Cost matrix

	Urban	Green	Water	Other
Weights 1	1	0.75	0.25	0.50
Weights 2	1	0.50	0.25	0.75

The Kappa statistic and Accuracy are the most common measures used to validate such models (Mondal et al, 2016). Accuracy is the ratio of the number of pixels that were predicted correctly to the total number of pixels. We used PLUS to predict land use maps for Chennai in 2017 and Bengaluru in 2020 based on the transition matrices generated (using base land use maps from 1997 and 2009 for Chennai and 2011 and 2016 for Bengaluru) and input variables and compared these with the actual maps for these years. Tables 5-6 display the accuracy with which we were able to predict the land cover in Chennai in 2017 and in Bengaluru in 2020.

Table 5. Accuracies for Chennai

Case	Accuracy	Kappa
1.1	76.33	0.6695
1.2	76.04	0.6652
2.1	76.07	0.666
2.2	76.12	0.6663

Table 6. Accuracies for Bengaluru

Case	Accuracy	Kappa
1.1	68.43	0.5226
1.2	68.34	0.521
2.1	67.83	0.5132
2.2	68.22	0.5194

The explanatory variables (input variables) were iteratively used to see which combinations provided the best results. Often, a lot of mismatches happen at the outer edges of the urban area. An alternative that we explored was to resize the map and focus more on the central portion of these cities. Hence, a new set of maps which are 75% of the size of the original maps were made and the same models were run again. There was no significant improvement in accuracies and kappa values when this resized map was used. These levels of accuracy ranging between 67% and 77% show that the predictive power of the model is acceptable but also indicate that changes in between time periods are not necessarily predicated on trends experienced in previous time periods and that urbanization and land cover change happen at differing rates over time.

Having established the usability of the model, we next turned to the process of incorporating UPA and farming as a land cover category in these maps.

4. Understanding the growth of UPA in Chennai and Bengaluru

The land cover categories that we used – urban built-up, water, green and other, were not granular enough to allow us to understand the spread of UPA. For instance the proportion of urban built-up areas that constituted rooftop gardens or practiced terrace farming could not be derived from the satellite data. Therefore to integrate the growth of UPA into the larger LULC simulations of Chennai and Bengaluru, we conducted a survey to identify specific trends related to UPA. Once identified, these trends could then be integrated into our model as described below. The purpose of the survey undertaken in the Chennai and Bengaluru region was to understand the number and type of people who are engaged in urban farming, the activities that they performed and temporal shifts in the amount of urban farming undertaken. The data collected in the survey can be broken into the following categories:

1. Location data to understand where people are engaged in urban farming
2. Personal data to understand their demographics better.
3. The extent of farming activities: area of farm/garden, kinds of plants and trees
4. Farming practices and experience: type of farm, mode of farming, how long they have been engaged in farming, earlier land cover type, increase or decrease in the size of their farms.
5. Future plans: likelihood of continuing with urban farming or not, future increase/decrease in area, likely area of new garden/farm, what type of area will people use.

The survey was made available both digitally and in print and a publicity campaign was undertaken to encourage citizens from Chennai and Bengaluru to fill in the survey. We then extracted the following types of data from the survey:

1. Number of people currently engaged in UPA
2. Location- Where UPA farms were located, types of land cover that were being converted into UPA.
3. Average area of a garden/UPA farm
4. Increase/decrease in UPA area per year in the past.
5. The kinds of plants and produce that were being grown as well as the means of growing (e.g. pots, baskets, or ground).
6. Respondents' aspirations for the future in terms of expanding, contracting or maintaining their farms
7. UPA growth factor based on the number of new people who have taken to urban farming in previous years.

We created a new fifth category in our land cover classification called 'farming' to denote the extent of area where UPA was being undertaken. Two tasks were undertaken. The first was to estimate the total number of pixels that could be attributed to farming, and the second was to distribute these pixels on the map. While our data was able to help us understand the average UPA farm holding size, the kinds of crops grown and the rate at which UPA farms such as terrace gardens were likely to grow (based on respondents answers to questions regarding whether they planned to start up, expand, decrease or maintain UPA areas in the future as well as data on past trends such as when they had started farming and how they have expanded in the past) we did not have sufficient data on the percentage of the population that was engaged in UPA at the current time. As a result, three scenarios were taken into consideration:

- Scenario 1: When 1.5% of total households are engaged in farming
- Scenario 2: When 2.5 % of total households are engaged in farming
- Scenario 3: When 3.5 % of total households are engaged in farming

These scenarios were selected based on an estimate of the proportion of people in a city likely to be engaged in UPA. Based on the above scenarios, the number of farming pixels for

Chennai and Bengaluru were calculated and pixels from other land cover categories were replaced with these farming pixels on the map. In the case of Bengaluru, the average area of farming land per person was found to be 11,796.78 sq. feet in 2016 and 12,596.47 sq. feet in 2020 based on the survey collected. This data coupled with the percentage of the population engaged in farming, a 3% annual growth rate of UPA that we obtained from our survey, as well as the 30mx30m dimension of each pixel allowed us to calculate the number of farming pixels in our map for 2016 and 2020 under each of the three scenarios The number of farming pixels for Bengaluru is represented in Table 7 below.

Table 7. Bengaluru Scenarios for modeling

Scenarios	Farming Pixels- 2016	Farming Pixels- 2020
When 1.5% of total households are engaged in farming	42718	54444
When 2.5% of total households are engaged in farming	71362	87925
When 3.5% of total households are engaged in farming	102984	129508

In the case of Chennai, the average farming land per person was found to be 686.145 sq. feet for the year 2020. Since the extent of UPA in Chennai appeared to be lower than that in Bengaluru the three scenarios for Chennai involved 1%, 2% and 3% of the population undertaking UPA respectively. A growth factor of 3%, similar to that in Bengaluru was taken into consideration. Given the relatively smaller landholdings for UPA in Chennai, we first assumed that an area of a minimum of one pixel on our map was used by each urban farmer. This was then used to calculate the total area and consequently the number of pixels of urban farming in our map under each of the three scenarios. This is depicted in Table 8.

Table 8. Chennai Scenarios for modeling

Scenarios	Farming Pixels in 2009	Farming pixels in 2017
1% of total households are engaged in farming	18967	24042
2% of total households are engaged in farming	38327	48434
3% of total households are engaged in farming	58460	72231

Image processing and reclassification

Having arrived at an estimate of the extent of UPA in Chennai and Bengaluru, our next task was to distribute these landholdings on our existing maps. NDVI images acquired from online resources proved helpful in reclassifying pixels from other land use categories into farming. Satellite images from LANDSAT 5, LANDSAT 7 and LANDSAT 8 were downloaded from the United States Geological Survey's (USGS) – Earth Explorer website. These consisted of maps in the visible and IR range spectrum, which helped calculate the NDVI and LST.

The NDVI map ranges varied from -1 to 1. The NDVI range for urban farming was selected based on the survey data collected: The data indicated that more than 90% (91.11%) of the farming pixels were earlier a part of urban built-up area while the remaining pixels were part of the 'other' category. From this information, we selected an NDVI range from the tail-end of values for urban built-up space to the start of vegetation (0.055 to 0.08 in Bengaluru and 0.0725 to 0.1 for Chennai). Once this was done, farming pixels were randomly placed in cells which fit this NDVI range subject to the constraints from Tables 7 and 8. Based on these assumptions, the four land cover categories maps were converted to 5 land cover categories maps for each scenario.

5. Predicting Future Scenarios for UPA

Based on the six scenarios discussed in the previous section (3 each for Bengaluru and Chennai), future land cover maps were predicted using Markov Chain analysis. Maps with 5 land use categories (including urban farming) were first created for 2009 and 2017 for Chennai, and 2016 and 2020 for Bengaluru as described in the previous section. 5x5 transition matrices for both Chennai and Bengaluru were then obtained by comparing these two maps. Transitions between other categories not involving urban farming (built-up to vegetation for instance) as well as the influence of the other input variables remained similar to those in the original 4x4 transition matrices that had been validated. These new 5x5 matrices were used for future predictions. The base model was run until 2032 in the case of Bengaluru and 2041 in the case of Chennai. Tables 9 and 10 depict the transition matrices that were used.

Table 9: Transition Matrices for Bengaluru

scenario 1: 1.5% of households engaged in farming					
2016-2020	built-up	vegetation	water	other	farming
built-up	0.989151	0	0	0	0.010849
vegetation	0.132913	0.46089	0.006229	0.399469	0.000498
water	0.085949	0.141962	0.553494	0.216408	0.002187
other	0.13529	0.136322	0.003911	0.723248	0.001228
farming	0	0	0	0	1

scenario 2: 2.5% of households engaged in farming					
2016-2020	built-up	vegetation	water	other	farming
built-up	0.984949	0	0	0	0.015051
vegetation	0.132488	0.461323	0.006167	0.399418	0.000604
water	0.085562	0.142677	0.55176	0.216266	0.003735
other	0.13486	0.136664	0.003864	0.723034	0.001578
farming	0	0	0	0	1
scenario 3: 3.5% of households engaged in farming					
2016-2020	built-up	vegetation	water	other	farming
built-up	0.974154	0	0	0	0.025846
vegetation	0.13194	0.461722	0.006034	0.399351	0.000953
water	0.084802	0.143555	0.54867	0.215295	0.007678
other	0.134286	0.137043	0.003731	0.722299	0.002641
farming	0	0	0	0	1

Table 10: Transition matrices for Chennai

scenario 1: 1% of households engaged in farming					
2009-2017	built-up	vegetation	water	other	farming
built-up	0.993797	0	0	0	0.006203
vegetation	0.09937	0.521834	0.009501	0.368714	0.000581
water	0.00302	0.017185	0.958059	0.021571	0.000165
other	0.112617	0.313315	0.012698	0.55985	0.00152
farming	0	0	0	0	1
scenario 2: 2% of households engaged in farming					
2009-2017	built-up	vegetation	water	other	farming
built-up	0.987705	0	0	0	0.012295
vegetation	0.098791	0.522271	0.009397	0.368392	0.001149
water	0.002951	0.017061	0.958309	0.021235	0.000445
other	0.111439	0.314285	0.012634	0.55869	0.002952
farming	0	0	0	0	1
scenario 3: 3% of households engaged in farming					
2009-2017	built-up	vegetation	water	other	farming
built-up	0.983744	0	0	0	0.016256
vegetation	0.098248	0.522849	0.009262	0.368038	0.001603
water	0.002871	0.016908	0.958659	0.020848	0.000714
other	0.110218	0.31515	0.012511	0.557941	0.00418
farming	0	0	0	0	1

For the Bengaluru region, using transition matrices generated from the 2016 and 2020 maps, the future land cover distributions in pixels were estimated for years 2024, 2028, and 2032 for all three scenarios. Similarly, in the case of Chennai, the future land cover distributions in pixels were estimated for years 2025, 2033, and 2041. Tables 11 and 12 depict this distribution for Bengaluru in 2024 and Chennai in 2025 while Figures 3 and 4 show these distributions spatially with urban farming now included as a category.

Table 11. Pixel Distribution in Bengaluru in 2024

	Bengaluru					
	year	urban	green	water	other	farming
Scenario 1 (1.5%)	2020	1253211	914569	38027	1739527	54666
	2024	1599782	664051	33549	1631681	70938
	2028	1894320	533252	29088	1452639	90702
	2032	2143671	447927	25103	1269931	113368
	year	urban	green	water	other	farming
Scenario 2 (2.5%)	2020	1225624	914336	37618	1735127	87295
	2024	1565533	664301	33100	1627894	109173
	2028	1852351	533654	28650	1449514	135830
	2032	2093107	448371	24700	1267395	166427
	year	urban	green	water	other	farming
Scenario 3 (3.5%)	2020	1190060	914037	36885	1729510	129508
	2024	1515277	664343	32205	1622187	165988
	2028	1784336	533674	27730	1443944	210316
	2032	2004885	448272	23821	1262053	260968

Table 12. Pixel Distribution in Chennai in 2025

	Chennai					
	year	urban	green	water	other	farming
Scenario 1 (1%)	2017	631487	825237	1652544	991621	24072
	2025	826238	769725	1603667	895083	30248
	2033	1003246	709670	1555086	819514	37445
	2041	1164531	653820	1507013	754015	45583
	year	urban	green	water	other	farming
Scenario 2 (2%)	2017	616631	823398	1651562	984936	48434
	2025	805028	767765	1602887	888677	60604
	2033	974742	707626	1554503	813370	74721
	2041	1127893	651723	1506619	748114	90611
	year	urban	green	water	other	farming
Scenario 3 (3%)	2017	602373	821456	1650277	978624	72231
	2025	785887	765814	1601906	882747	88608
	2033	950244	705688	1553819	807767	107443
	2041	1097621	649808	1506225	742801	128506

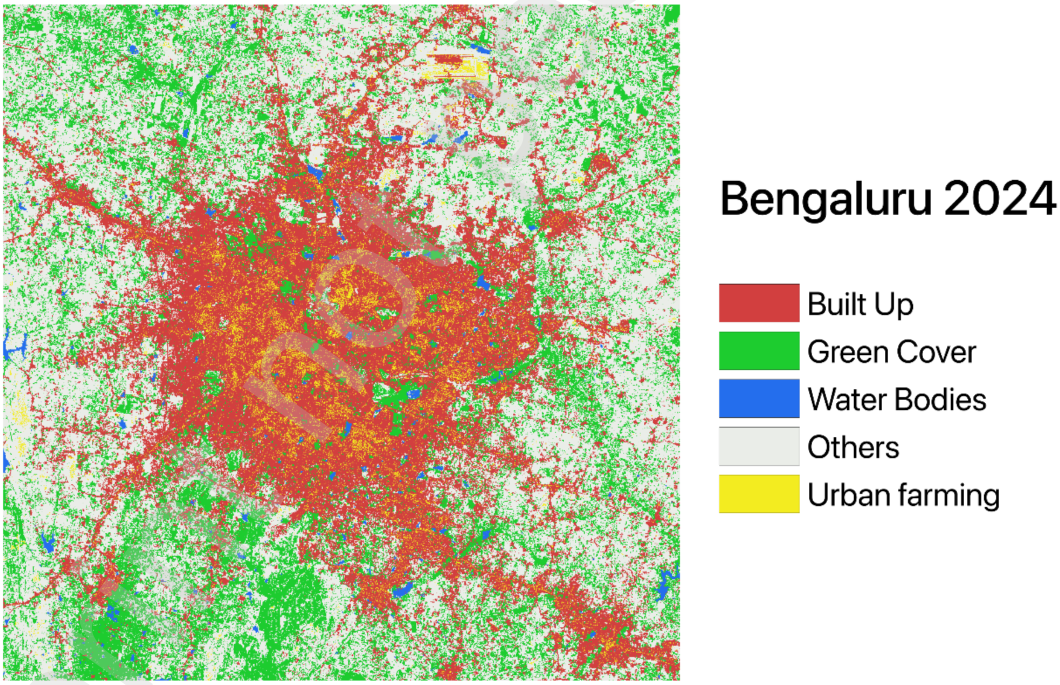

Figure 3. Predicted Land Cover map of Bengaluru in 2024

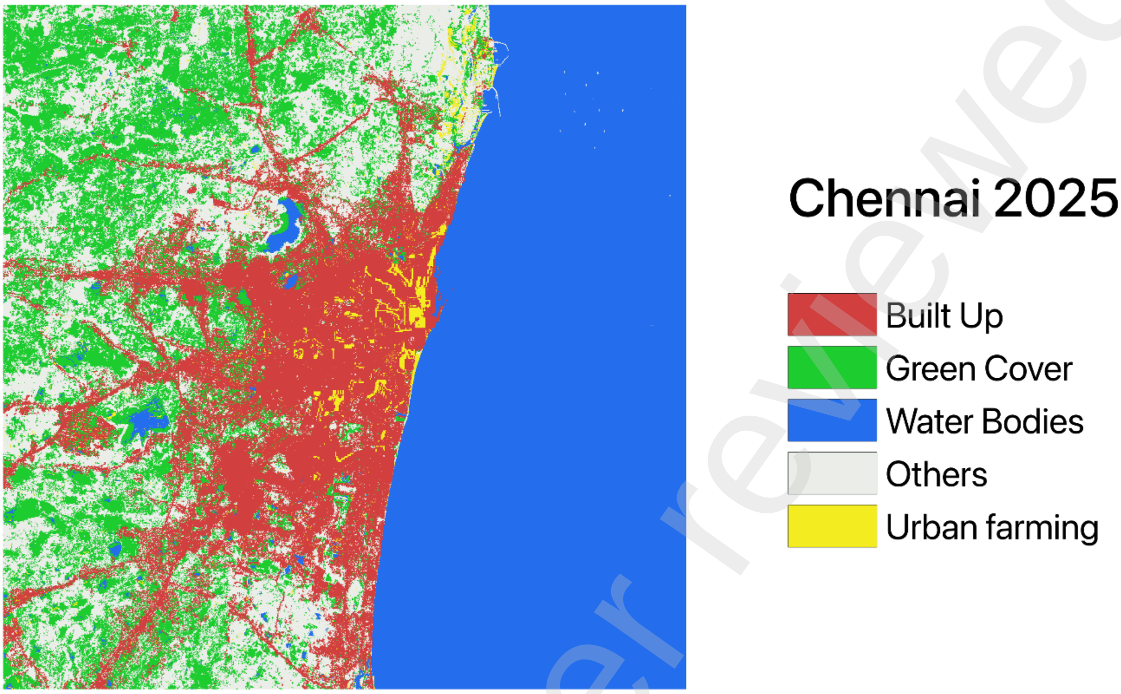

Figure 4. Predicted Land Cover map of Chennai in 2025

6. Analyzing the impact of UPA

After simulating the urban farming growth in terms of area, our next step was to quantify this growth in terms of impact. As discussed earlier, three metrics - carbon stock estimation, NDVI and LST are used to quantify the impacts of growth in urban and peri-urban agriculture.

Carbon stock estimation

Carbon stock is the amount of carbon available in the form of biomass, soil, deadwood, litter etc. The higher the carbon stock is, the higher will be the ability of the region to sequester CO_2. Afforestation is one of the indirect methods used to sequester CO_2. Hence, a growth in urban and peri-urban agriculture will also lead to an increase in the carbon sequestration potential in urban areas. One of the traditional ways to calculate the carbon stock is by estimating the biomass present in the trees and plants and then using a conversion factor to convert it into carbon stock (Petrokofsky et al, 2012). Traditionally, biomass is estimated through practical ways where measurements are made for the trees growing in a parcel of land. Then based on the wood densities and other factors such as a crop coefficient, the biomass is calculated. For the present study, the types of plants grown are estimated and based on their distribution, the biomass values (per unit area) for similar vegetation are taken from existing literature in order to calculate the total biomass content in each city that is contributed by UPA. The survey data provides insights into the types of trees that are grown and also the size of the farm. By combining this data and the values of biomass from external studies, we arrived at an estimate of the available total biomass.

From the survey we observed that 50% of the farms are sub-300 sq.ft., 20% are more than 1000 sq. ft. and the remaining 30% are in between. 24% of the responses mentioned an increase in the farm area over time, 12% suggested that farm areas had decreased and for 64% the farm size remained the same. We assumed that the larger farms have fruit trees and benchmarked them with mango and orange trees, while we assumed the small and medium farms had a mix of plants and trees. Two cases/scenarios are assumed where the composition of vegetation varies slightly across farm categories. The types of vegetation that we considered in each case are shown in Table 13. Typical plants in these categories and their corresponding biomass values for these kinds of vegetation are shown in Table 14.

Table 13: Cases and vegetation types

	Farm size	Type of plant / tree grown
Case 1	<300	50% flowering, 50% herbs
	300 to 1000	100% vegetables
	>1000	50% mango, 50% orange
Case 2	<300	50% flowering, 50% herbs
	300 to 1000	25% each of mango & orange, 40% of vegetables, 10% flowering
	>1000	45% each of mango & orange, 10% flowering

Table 14. Biomass values

Plant	Biomass(kg/m2)
Rose / flowering plants	1.3
Orange	1.731
Mango	2.691
coriander	0.161
vegetables	1.8

Based on the build out till 2032 in Bengaluru and 2041 in Chennai, the number of farm holdings of each of the three sizes is estimated as a proportion of the total farming pixels. For each of these farmholding types, the carbon density was calculated using the case assumptions in Table 13 and the corresponding biomass values in Table 14 and aggregated to arrive at the aggregate tonnage of biomass that resulted due to UPA in these cities. Results for Chennai and Bengaluru are presented in the form of graphs in Figures 5 and 6. In each city we simulated 3 scenarios of varying initial populations engaged in UPA as discussed earlier along with two different configurations of plant mixes in the urban farms leading to 6 different cases in each city. The amount of biomass available increases over time as the models suggest growth in urban and peri urban farming. There is a 91% to 102% growth in biomass in the case of Bengaluru and an increase of 81% to 125% in the case of Chennai across the six scenarios.

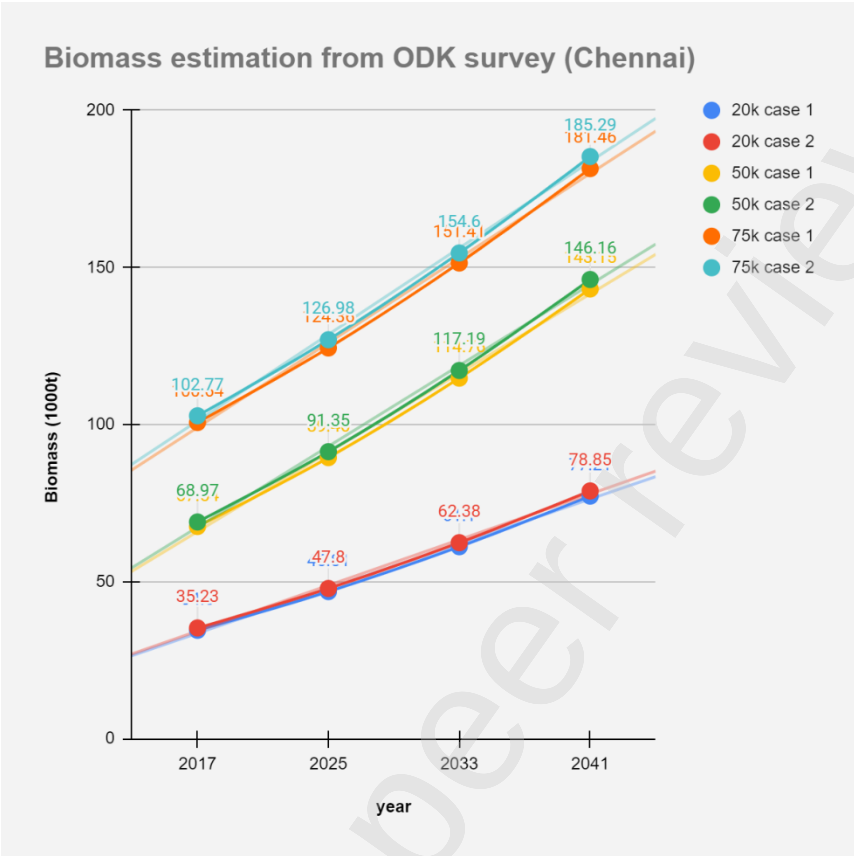

Figure 5. Estimated Biomass growth for Chennai due to UPA

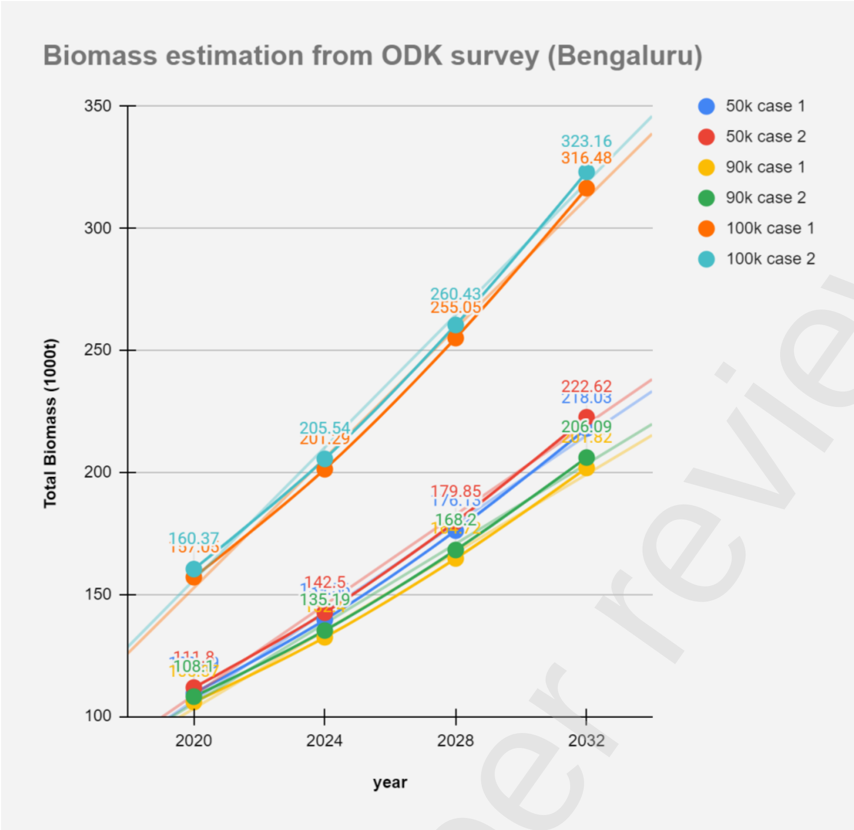

Figure 6. Estimated Biomass for Bengaluru due to UPA

Change in NDVI

Normalized Difference Vegetation Index (NDVI) is a simple vegetation index that identifies vegetation 'greenness' and is used in many different applications. The NDVI is an empirically derived index used to estimate plant biomass through the integration of the red–visible and near-infrared spectral regions to represent plant pigmentation and chlorophyll content respectively, in the characterization of land cover conditions. NDVI data were aggregated to pixels through a flat field aggregation approach in which each pixel contributed equally to the areally averaged value. We used the formula below:

$$NDVI = NIR - RED / NIR + RED \text{ (Ndossi and Avdan, 2016)}$$

where NIR is the near infrared brightness value, and RED is the red visible brightness value. The NDVI maps obtained from the satellite images have pixel values ranging from -1 to +1. A preliminary analysis on the change in mean NDVI values across the city reveals a net decrease in the mean NDVI over the last decade. This net change was -0.0488 for Chennai and -0.1575 for Bengaluru. A similar approach is used to predict the change in NDVI in future due to growth in urban and peri urban agriculture through the introduction of the 'farming' pixel category. Once the current year maps (2017 for Chennai and 2020 for Bengaluru) were reconstituted with 5 land cover types, the mean NDVI for each of the 5 categories was calculated using ArcGIS Pro. The results are shown in tables 15 and 16. Once the land cover distributions for the future were simulated, we performed a matrix multiplication with the average NDVI values of each land cover category to obtain the mean NDVI values for Chennai and Bengaluru.

Table 15. Final mean of NDVI range for 5x5 maps (Bengaluru)

2020 Bengaluru	Mean NDVI
Urban	0.1488
Green	0.2404
Water	0.068
Other	0.1738
farming	0.258

Table 16. Final mean of NDVI range for 5x5 maps (Chennai)

2017 Chennai	Mean NDVI
Urban	0.1405
Green	0.2654
Water	-0.0478
Other	0.1742
farming	0.2825

NDVI trends across the 3 scenarios in Chennai and Bengaluru are plotted in Figures 7 and 8 along with a fourth scenario that assumes no farming pixels and no UPA, to understand the contribution of UPA to NDVI. From the graphs, it can be inferred that the NDVI trend for Bengaluru differs from Chennai. There appears to be an improvement in average NDVI Chennai but a decline in Bengaluru over time indicating that the loss of vegetation due to urbanization in Bengaluru has a greater impact on NDVI than the increase due to UPA. Irrespective of the NDVI trend however, the mean NDVI saw an improvement as the urban farming area increased. However, the improvement is miniscule (~0.01).

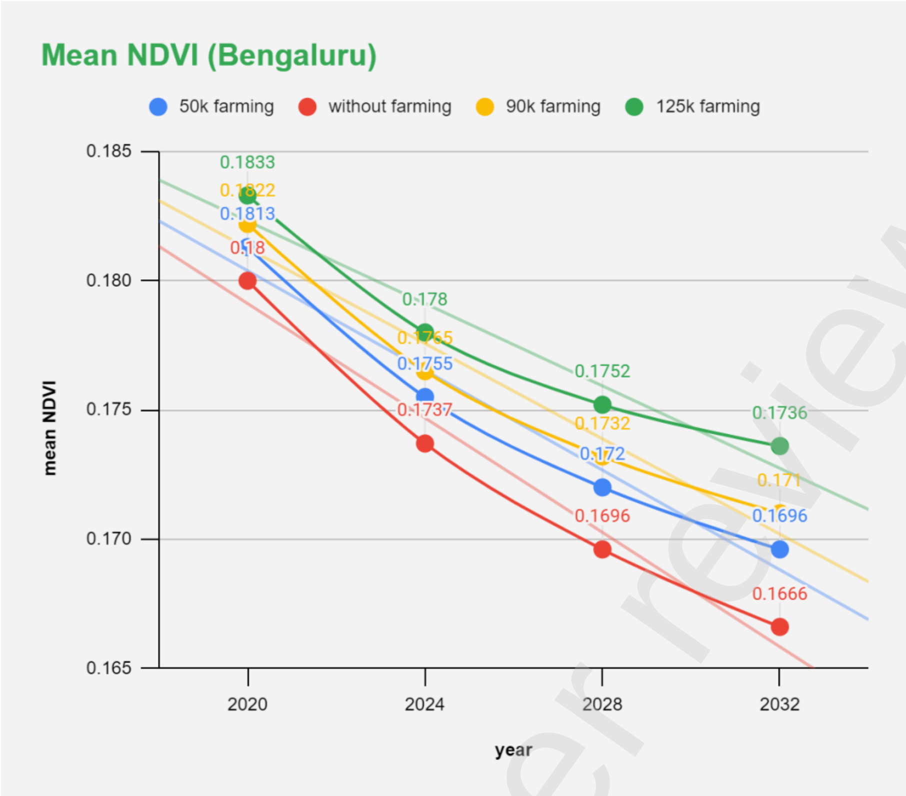

Figure 7. Change in Mean NDVI (Bengaluru)

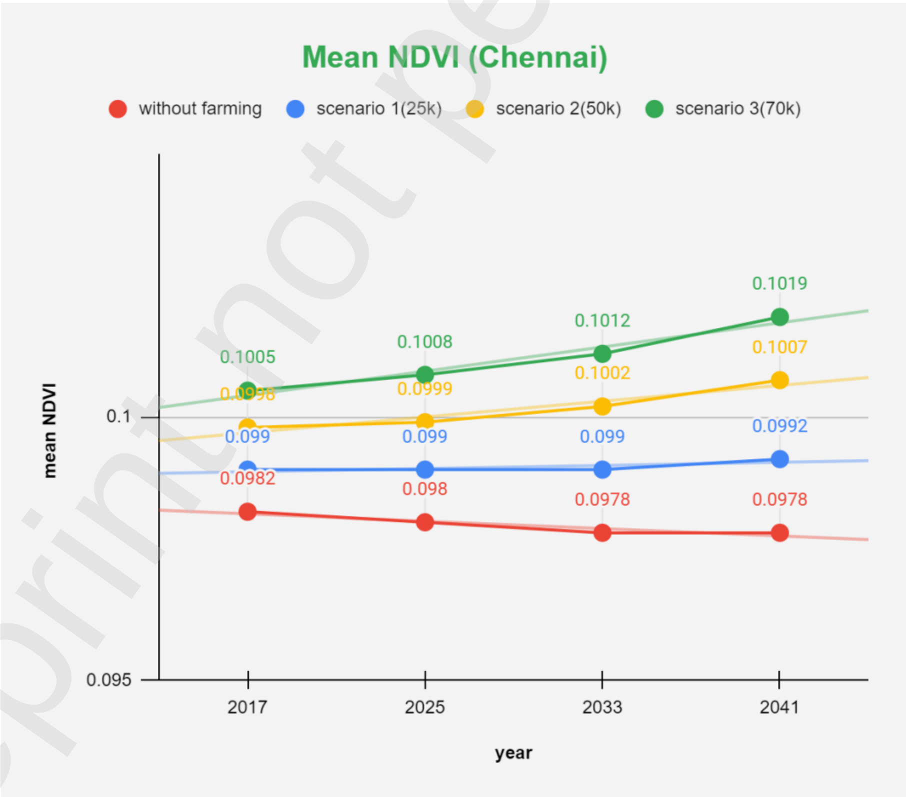

Figure 8. Change in Mean NDVI (Chennai)

Change in LST

"Urban heat islands" (UHI) occur when cities replace natural land cover with dense concentrations of pavement, buildings, and other surfaces that absorb and retain heat. This effect increases energy costs (e.g., for air conditioning), air pollution levels, and heat related illness and mortality. Weng and Yang (2006) in their work on urban air pollution patterns, land use, and thermal landscape note that the relationship between air pollution and urban heat (and thus UHIs) is not clearly understood, although both are related to the pattern of urban land use and land cover. UHIs may affect air pollution (Ward and Baleynaud, 1999) and higher urban temperatures may generally result in higher ozone levels as well (DeWitt and Brennan, 2001). Higher urban temperatures may also lead to increased energy use, as air conditioning requirements increase. Consequently this could lead to an increased use of fossil fuels as well. The temperature for UHI calculation is different from the air temperatures which are typically measured by weather stations. The UHI is estimated through Land Surface Temperature (LST). The satellite used for NDVI calculations also have the band 11 maps (part of the visible spectrum that gives the infrared maps) that were used for calculating LST.

The calculation is done using the following formula (see Ndossi and Avdan, 2016)-

$$LST = (BT / (1 + (0.00115 * BT / 1.4388) * Ln(\varepsilon)))$$

$$\text{Where, } TOA\ (L) = ML * Qcal + A$$

$$BT = (K_2 / (\ln (K_1 / L) + 1)) - 273.15$$

$$P_v = ((NDVI - NDVI_{min})/(NDVI_{max} - NDVI_{min}))\text{^}2$$

$$\varepsilon = 0.004 * Pv + 0.986$$

ε = emissivity, $\mathbf{P_v}$ = proportion of vegetation,

TOA = Top of atmosphere spectral radiance

BT = Brightness Temperature

$\mathbf{Q_{cal}}$ = corresponds to band 10.

$\mathbf{A_L}$ = Band-specific additive rescaling factor from the metadata (RADIANCE_ADD_BAND_x, where x is the band number).

$\mathbf{M_L}$ = Band-specific multiplicative rescaling factor from the metadata (RADIANCE_MULT_BAND_x, where x is the band number).

$\mathbf{K_1}$ = Band-specific thermal conversion constant from the metadata (K1_CONSTANT_BAND_x, where x is the thermal band number).

$\mathbf{K_2}$ = Band-specific thermal conversion constant from the metadata (K2_CONSTANT_BAND_x, where x is the thermal band number).

Since LST is a function of NDVI, mean LST values are estimated for the entire city for the various scenarios including the baseline scenario of no UPA, based on the NDVI data. Values for Bengaluru in 2020 and Chennai in 2017 are presented in tables 17 and 18 below.

Table 17. Mean LST Values in Bengaluru

2020 Bengaluru	Mean LST
Urban	34.49
Green	34.38
Water	29.2
Other	36.75
farming	29.34

Table 18. Mean LST Values in Chennai

2017 Chennai	Mean LST
Urban	36.11
Green	34.75
Water	26.48
Other	37.44
farming	33.86

We then calculated the Mean LST values from 2020 to 2032 in Bengaluru and from 2017-2041 in Chennai. The results are shown in Figures 9 and 10. Similar to the mean NDVI the mean LST in both the cities follows a certain trend due to their geography and local conditions. While mean LST in Bengaluru appears to decrease over time, mean LST in Chennai shows an almost monotonic increase. These values are also a function of the geographic location of these cities as well as the urbanization that is taking place. However, it can be inferred from the graph that by increasing the amount of land under urban farming there is a 0.15^0C reduction in LST in Bengaluru and in the future this improves to a 0.35^0C reduction. Similarly in the case of Chennai there is a reduction from 0.04^0C to 0.07^0C in land surface temperature across scenarios that is attributable to urban farming.

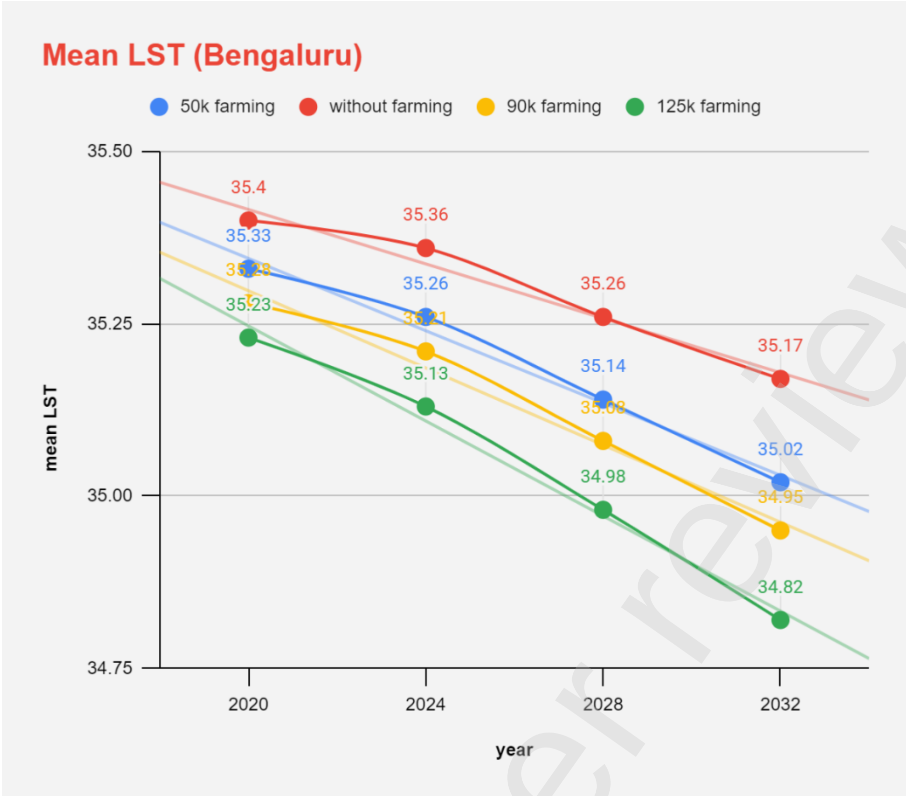

Figure 9. Change in Mean LST(Bengaluru)

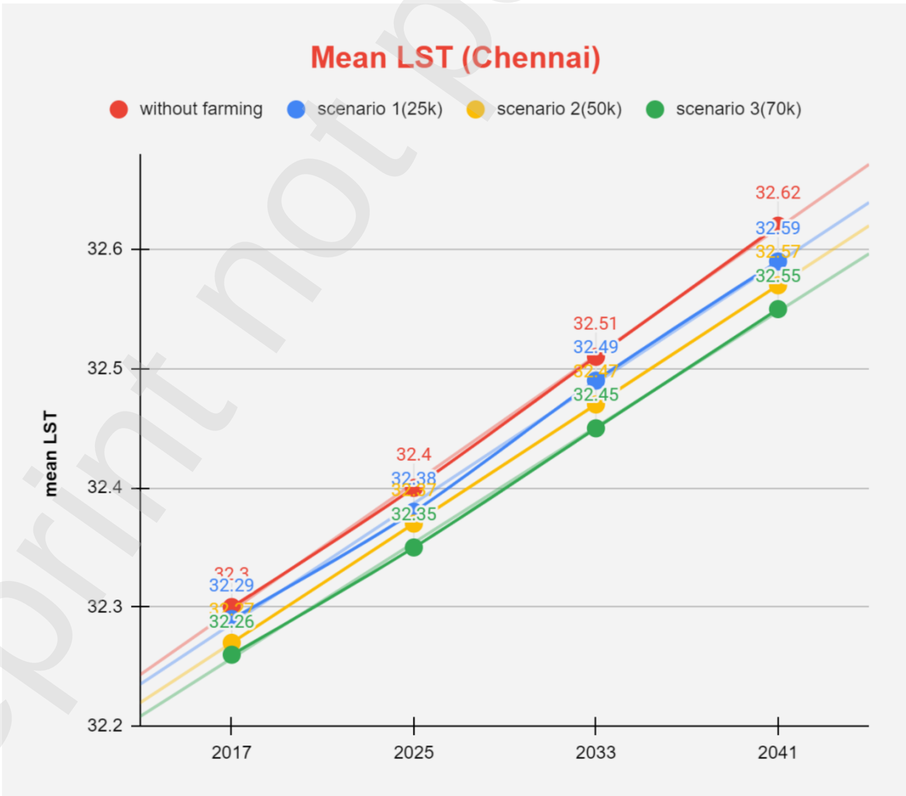

Figure 10. Change in Mean LST(Chennai)

7. Discussion and Conclusion

Our simulations indicate a drastic change in built-up land over time in both Chennai and Bengaluru. The built-up land went from 16% in 2011 to 32% in 2020 in Bengaluru and a similar pattern was seen in the case of Chennai. Furthermore, the transition matrices indicated that urban areas rarely change to other land cover types while water bodies and vegetation are likely to change to urban and other uses over time. The matrices also indicate that in some cases this change is bi-directional. For instance vegetation area is converted to barren land and some percentage of barren land is then converted to vegetation due to agriculture and afforestation.

The biomass available due to urban farming is the extra biomass available for the city, which can sequester CO from the atmosphere. The amount of carbon sequestered can be found out from biomass with the help of certain stoichiometric equations such as the following (Chavan and Rasal, 2012):[1].

$$\begin{aligned}\text{Amount of carbon} &= 0.5 * \text{Biomass}\\ \text{Carbon sequestered} &= 3.67 * \text{Carbon}\\ &= 0.5 * 3.67 * \text{Biomass}\\ &= 1.835 * \text{Biomass}\end{aligned}$$

Hence, the minimum amount of biomass attributable to UPA in Bengaluru is around 69,000 tons, leading to around 126,615 tons of CO_2 sequestered by all the urban farming that existed until 2020. The highest level of biomass in the future was around 140,000 tons, leading to the ability to sequester 256,900 tons of CO_2. Therefore, the growth of urban farming from 2020 to 2032 in Bengaluru can lead to a minimum of 130,285 tons of extra CO_2 sequestered assuming that only 1% of the population is indulging in urban farming today. These numbers are quite significant. In addition the extra biomass from all these plants and trees also serves as biofuel, organic fertiliser, fodder and so on.

The mean NDVI values showed a decreasing trend in Bengaluru and a slightly increasing trend in Chennai. The faster growth rate of urban areas in Bengaluru (102% increase in 9 years – 2011 to 2020) compared to Chennai (54.26% increase in 9 years – 2009 to 2017) could be one reason. Even in the case of Chennai, the most significant improvement across a 24 year timeframe is 0.0014, assuming 3% of the population is undertaking UPA activities. This indicates that UPA does not contribute significantly to a change in NDVI.

The mean LST values showed a decreasing trend in Bengaluru and an increasing trend in Chennai. It is safe to assume that the reasons for this trend are intrinsic to the topography of the respective cities. Concerning urban farming, the minimum decrease in mean LST is 0.17^0C in Bengaluru (when comparing the 3.5% scenario with the absence of UPA in 2020) and 0.14^0C in Chennai (when comparing the 3% scenario with the absence of UPA in 2017). The increase in LST is estimated at 0.3^0C in Chennai (2017 to 2041) while the decrease in

[1] https://www.unm.edu/~jbrink/365/Documents/Calculating_tree_carbon.pdf

LST is estimated at 0.31^{0}C to 0.41^{0}C in Bengaluru (2020 to 2032). While these numbers seem small in absolute terms, our results indicate that there is likely to be a significant localized difference in temperatures where urban farming is practiced.

Our work contributes to our understanding of UPA in two distinct ways. Our first contribution is methodological. The use of remote sensing and CA-Markov modeling has been commonplace in the area of land-use studies. We show that these methods can be used to study and quantify the impacts of UPA as well. We combine LULC analysis techniques with survey data to capture ground realities, and scientific formulations to determine the impact of UPA over time on parameters related to land surface temperature and the ability to sequester carbon. By bringing in and integrating techniques from diverse fields we show how spatial and temporal aspects of UPA can be studied and measured. This innovative approach opens up avenues of research that can supplement traditional qualitative or micro-quantitative studies and can help us estimate the overall impact of UPA on a number of parameters.

Our second contribution is towards our understanding of the impact of UPA and its bearing on policy development. Qualitatively the positive effects of UPA are well documented. Our models indicate that the impacts of UPA in terms of carbon density and the ability to sequester carbon are small, but non-negligible. Similarly, while UPAs impact on NDVI is minimal, we expect to see non-trivial impacts on LST at least at a localized level. Such findings can help policymakers determine whether to set policies and metrics around UPA growth and if so what these levels could be.

We acknowledge that our study is limited by several assumptions that we have made. Other explanatory variables may have increased the accuracy of our models. However, we believe that our urbanization estimates and therefore our estimates of UPA growth are on the conservative side and are likely to be higher in practice than what our models suggest. Larger surveys may help us peg the levels of current UPA practice more accurately and reduce the need for creating multiple scenarios. We believe that these limitations can be overcome in future work. Our primary goal in this paper was to demonstrate an integrated approach that combines remote sensing techniques with primary data to quantify and estimate the impacts of UPA. Our findings show that such integration is both possible and beneficial to our understanding of UPA benefits and impacts. We invite other researchers to join us to help refine and fine-tune our approach by building more accurate land cover simulations in the UPA context, collecting sharper data on UPA trends on the ground and exploring the impact of UPA on other variables such as air quality and livelihoods. In the process we hope to catalyze the creation of more sustainable urban spaces.

8. References

1. Arsanjani, J. J., Helbich, M., Kainz, W., & Boloorani, A. D. (2013). Integration of logistic regression, Markov chain and cellular automata models to simulate urban expansion. *International Journal of Applied Earth Observation and Geoinformation*, *21*, 265-275.

2. Asomani-Boateng, R. and Haight, M., (1999). Reusing organic solid waste in urban farming in African cities: a challenge for urban planners. Third World Plan. Rev. 21, 411–428.
3. Belsky AJ, Mwonga SM and Duxbury JM. (1993). Effects of widely spaced trees and livestock grazing on understory environments in tropical savannas. *Agrofor Syst* 24: 1–20
4. Chavan, B. L., & Rasal, G. B. (2012). Carbon sequestration potential and status of peltophorum pterocarpum (DC.) K. Heyne. *Science Research Reporter*, *2*(1), 51-55.
5. Corburn, J. (2009). Cities, climate change and urban heat island mitigation: localizing global environmental science. *Urban Stud*. 46, 413–427.
6. Di Leo, N., Escobedo, F. J., & Dubbeling, M. (2016). The role of urban green infrastructure in mitigating land surface temperature in Bobo-Dioulasso, Burkina Faso. *Environment, development and sustainability*, *18*(2), 373-392.
7. Drescher, A.W (2002) Food for the cities: urban agriculture in developing countries, in: *International Conference on Urban, Horticulture* 643, pp. 227–231.
8. Feng, H., Zhao, X., Chen, F., & Wu, L. (2014). Using land use change trajectories to quantify the effects of urbanization on urban heat island. *Advances in Space Research*, *53*(3), 463-473.
9. Guan, D., Li, H., Inohae, T., Su, W., Nagaie, T., & Hokao, K. (2011). Modeling urban land use change by the integration of cellular automaton and Markov model. *Ecological Modelling*, *222*(20-22), 3761-3772.
10. Hamad, R., Balzter, H., & Kolo, K. (2018). Predicting land use/land cover changes using a CA-Markov model under two different scenarios. Sustainability, 10, 3421.
11. Hua, A. K. (2017). Application of Ca-Markov model and land use/land cover changes in Malacca River Watershed, Malaysia. *Applied Ecology and Environmental Research*, *15*(4), 605-622.
12. Huang, J., Wu, Y., Gao, T., Zhan, Y., & Cui, W. (2015). An integrated approach based on Markov Chain and cellular automata to simulation of urban land use changes. *Applied Mathematics & Information Sciences*, *9*(2), 769.
13. International Development Research Centre (Canada), (2011). International Potato Center, (ed.), *African Urban Harvest: Agriculture in the Cities of Cameroon, Kenya, and Uganda,* Fountain. Fountain Publishers, International Development Research Centre; International Potato Centre, Kampala, Ottawa, Canada, Lima, Peru.
14. Kafy, A., Hossain, M., Prince, A. A. N., Kawshar, M., Shamim, M. A., Das, P., & Noyon, M. E. K. (2019). Estimation Of Land Use Change To Identify Urban Heat Island Effect On Climate Change: A Remote Sensing Based Approach. In *International Conference On Climate Change (Iccc-2019)*.
15. Ku, C. A. (2020). Exploring the Spatial and Temporal Relationship between Air Quality and Urban Land-Use Patterns Based on an Integrated Method. *Sustainability*, *12*(7), 2964.
16. Lee-Smith, D., (2010). Cities feeding people: an update on urban agriculture in equatorial Africa. *Environ. Urban*. 22, 483–499.
17. Li, X., & Yeh, A. G. O. (2002). Neural-network-based cellular automata for simulating multiple land use changes using GIS. *International Journal of Geographical Information Science*, *16*(4), 323-343.
18. Liang, X., Guan, Q., Clarke, K. C., Liu, S., Wang, B., & Yao, Y. (2021). Understanding the drivers of sustainable land expansion using a patch-generating land use simulation

(PLUS) model: A case study in Wuhan, China. *Computers, Environment and Urban Systems*, *85*, 101569.

19. Liu, X., Liang, X., Li, X., Xu, X., Ou, J., Chen, Y., ... & Pei, F. (2017). A future land use simulation model (FLUS) for simulating multiple land use scenarios by coupling human and natural effects. *Landscape and Urban Planning*, *168*, 94-116.
20. Liu, X., Wang, S., Wu, P., Feng, K., Hubacek, K., Li, X., & Sun, L. (2019). Impacts of urban expansion on terrestrial carbon storage in China. *Environmental science & technology*, *53*(12), 6834-6844.
21. Lwasa, S., Mugagga, F., Wahab, B., Simon, D., Connors, J., & Griffith, C. (2014). Urban and peri-urban agriculture and forestry: Transcending poverty alleviation to climate change mitigation and adaptation. *Urban Climate*, *7*, 92-106.
22. Macdonald, D., Dixon, A., Newell, A., & Hallaways, A. (2012). Groundwater flooding within an urbanised flood plain. *Journal of Flood Risk Management*, *5*(1), 68-80.
23. Masashua, H.E., Provident, J., Hawassi, G., (2009). *Potentials of urban horticulture for poverty reduction in Dar es salaam: the case of Kinondoni Municipality*. Eldis, Poverty Resource Guide (Online).
24. Mitsova, D., Shuster, W., & Wang, X. (2011). A cellular automata model of land cover change to integrate urban growth with open space conservation. *Landscape and urban planning*, *99*(2), 141-153.
25. Mondal, M. S., Sharma, N., Garg, P. K., & Kappas, M. (2016). Statistical independence test and validation of CA Markov land use land cover (LULC) prediction results. *The Egyptian Journal of Remote Sensing and Space Science*, *19*(2), 259-272.
26. Ndossi, M.I, and Avdan, U. (2016). Application of open source coding technologies in the production of land surface temperature (LST) maps from Landsat: a PyQGIS plugin. *Remote sensing*, *8*(5), 413.
27. Nirupama, N., & Simonovic, S. P. (2007). Increase of flood risk due to urbanisation: A Canadian example. *Natural Hazards*, *40*(1), 25-41.
28. Oke, TR (1982). The energetic basis of the urban heat island. *Quarterly Journal of the Royal Meteorological Society*, 108, Pp 1-24
29. Parece, T. E., & Campbell Jr, J. B. (2017). Assessing urban community gardens' impact on net primary production using NDVI.
30. Petrokofsky, G., Kanamaru, H., Achard, F., Goetz, S. J., Joosten, H., Holmgren, P., Lehtonen, A., Menton, M, Pullin, A and Wattenbach, M. (2012). Comparison of methods for measuring and assessing carbon stocks and carbon stock changes in terrestrial carbon pools. How do the accuracy and precision of current methods compare? A systematic review protocol. *Environmental Evidence*, *1*(1), 1-21.
31. Plavnick, A. (2008). The fundamental theorem of markov chains. *University of Chicago VIGRE REU.*
32. Rimal, B., Zhang, L., Keshtkar, H., Haack, B. N., Rijal, S., & Zhang, P. (2018). Land use/land cover dynamics and modeling of urban land expansion by the integration of cellular automata and markov chain. *ISPRS International Journal of Geo-Information*, *7*(4), 154.
33. Ricci, L. (2012). Peri-urban livelihood and adaptive capacity: urban development in Dar Es Salaam. *J. Sustain. Dev*., 39–54

34. Vandenbeldt RJ and Williams JH. (1992). The effect of soil surface temperature on the growth of millet in relation to the effect of Faidherbia albida trees. *Agricultural and Forest Meteorology* 60: 93–100
35. Weng, Q. (2001). A remote sensing? GIS evaluation of urban expansion and its impact on surface temperature in the Zhujiang Delta, China. *International journal of remote sensing*, *22*(10), 1999-2014.
36. Weng, Q., and Yang, S. (2006). Urban air pollution patterns, land use, and thermal landscape: an examination of the linkage using GIS. *Environmental monitoring and assessment*, *117*(1), 463-489.
37. Ward, L. and Baleynaud, J.-M.: (1999), Observing air quality over the city of Nates by means of Landsat thermal infrared data, *Int. J. Remote Sens.* 20(5), 947–959.